β93 Modified Hemoglobin: Kinetic and Conformational Consequences†

Imran Khan,‡ David Dantsker,‡ Uri Samuni,‡ Adam J. Friedman,‡ Celia Bonaventura,§ Belur Manjula,‡ Seetharama A. Acharya,‡ and Joel M. Friedman*,‡

Department of Physiology and Biophysics, Albert Einstein College of Medicine, Bronx, New York, 10461, and Marine/Freshwater Biomedical Center, 135 Duke Marine Lab Road, Beaufort, North Carolina 28516-9721

Received January 8, 2001; Revised Manuscript Received April 20, 2001

ABSTRACT: The reactive sulfhydryl on Cys β93 in human adult hemoglobin (HbA) has been the focus of much attention. It has purported functional roles such as a transporter of nitric oxide and a detoxifier of super oxide. In addition, it has a proposed role in the allosteric mechanism. The present study addresses the functional and conformational consequences of modifying the β93 sulfhydryl using either maleimide or disulfide-based reactions. The geminate and bimolecular recombination of CO derivatives of several different β93-modified Hbs in both solution and sol−gel matrixes provide a window into functional modifications associated with both the R and T states of these proteins. Nanosecond time-resolved visible resonance Raman spectroscopy is used to probe conformational consequences associated with the proximal heme environment. The results show functional and conformational consequences that depend on the specific chemistry used to modify β93. Maleimide-based modification show the most significant alterations of R-state properties including a consistent pattern of a reduced geminate yield and a loss of the favorable heme-proximal histidine interaction normally seen for liganded R-state HbA. A mechanism based on a displacement of the side chain of Tyr β145 is explored as a basis for this effect as well as other situations where there is loss of the quaternary enhancement effect. The quaternary enhancement effect refers to the enhancement of ligand binding properties of the $\alpha\beta$ dimers when they are associated into the R-state tetramer.

Hemoglobin (Hb)[1] functions as the primary oxygen transport protein in nearly all vertebrate organisms (*1*). More recently, other functions have been either identified or proposed for both vertebrate and nonvertebrate Hbs. Some of these proposed additional functionalities are based on the presence of reactive sulfhydryl groups. Each of the two Cys β93 residues in human adult Hb (HbA) has a reactive sulfhydryl group. These sulfhydryl groups, which are the only reactive ones in the tetramer, have been implicated in a number of reactions that have important functional consequences for HbA. Formation of an SNO derivative at β93 occurs to a limited extent in vivo and has been proposed (*2*, *3*) to play an important role in controlling vasoactivity. Direct evidence from spin resonance measurements suggests that β93 may also function as a deactivator of superoxide generated upon oxygen dissociation within the distal heme pocket (*4*). There are also indications of a redox linkage to the β heme (*5*). Furthermore, β93 modifications are being explored as a means of generating suitable candidates for clinically viable acellular oxygen transport reagents, such as $(PEG2000)_2$XLHbA (*6*) and anti-sickling forms of HbS, such as glutathionyl HbS (*7*, *8*). The objective of the present study is to better understand the conformational and functional consequences resulting from chemical modification of the β93 sulfhydryl group.

Cys β93 is situated in a conformationally plastic domain containing residues whose interactions are directly linked to allosteric properties of the Hb tetramer (*9*−*12*). The reactivity of the β93 sulfhydryl toward many reactants is highly sensitive to both the quaternary and tertiary conformation of HbA (*13*−*21*). It has been proposed that in vivo functional roles of β93 are also modulated by the overall protein structure (*2*). Conversely, modification of the β93 sulfhydryl has been shown to have an impact on both the allosteric properties of HbA and the ligand binding reactivity of HbA within a given quaternary state (*22*−*27*). Little is known regarding the molecular details of how the binding of reagents to β93 impacts Hb structure and function.

In the present study, two categories of β93 modification in HbA are probed in an attempt to further examine how ligand binding properties and protein conformation respond to these local perturbations. One category includes several derivatives generated through a maleimide reaction with the sulfhydryl (resulting in a relatively large and rigid succinimidyl group attached to β93). Within this group there are different substituents covalently attached to the succinimidyl group, ranging from small ethyl groups (NESHbA) to large poly(ethylene glycol) (PEG) chains connected through either a phenoxy or an ethoxy linker. The second category consists

† This supported was supported in part by the National Institutes of Health through Grants R01 HL58247, R01 HL58248, R01 HL65188, and GM58890 and by the W. M. Keck Foundation.

* To whom correspondence should be addressed. Phone: (718) 430 3591. Fax: (718) 430 8819. E-mail: jfriedma@aecom.yu.edu.

‡ Department of Physiology and Biophysics.

§ Marine/Freshwater Biomedical Center.

[1] Abbreviations: HbA, human adult hemoglobin; XLHb, crossbridged hemoglobin; IHP, inositol hexaphosphate; GSH, glutathione; 4-PDS, 4,4-dithiopyridine; NEM, *N*-ethylmaleimide; NES, *N*-ethylsuccinimide; NO, nitric oxide; CO, carbon monoxide; PEG, poly(ethylene glycol); GR, geminate recombination; GY, geminate yield.

10.1021/bi010051o CCC: $20.00 © 2001 American Chemical Society
Published on Web 05/31/2001

of modifications in which molecular species (glutathione (GSH) and thiopyridone) are linked to β93 through a disulfide bond.

Ligand binding reactivity of β93-modified forms was monitored through the geminate and bimolecular recombination of CO that occurs after the nanosecond photodissociation of the CO saturated derivative. The local tertiary structure at the ligand binding site was monitored using resonance Raman as a probe of the conformation-sensitive bond between the iron and the proximal histidine.

Ligand rebinding kinetics (*28*−*31*) are an effective probe of functionality for sol−gel encapsulated Hbs as well as for Hb in solution. Kinetic traces can be generated quickly and the kinetic analysis allows for identification of functionally distinct populations. Ligand rebinding kinetics from photodissociated liganded Hbs fall into two classes of phenomena: a submicrosecond intraprotein rebinding termed geminate recombination (*31*−*36*) and a solvent phase bimolecular rebinding (*28*). Both are highly sensitive to conformation and solvent conditions.

In solution at ambient temperature the fraction of the photodissociated population undergoing geminate recombination, i.e., the geminate yield (GY) (*36*−*47*) and the rate of solvent recombination (*28*−*31*) are both dependent upon the protein conformation to which the ligand rebinds. In solution, geminate recombination can occur over a temporal window extending from a few picoseconds out to several hundred nanoseconds. This time scale is faster than the time scales for both quaternary relaxation (20 μs) and large amplitude tertiary relaxations ($\sim$1 μs) (*30*, *48*−*53*). Thus, for geminate recombination, the protein conformation that determines the GY may be presumed to reflect the tertiary and quaternary structure of the starting liganded species.

The rate constant for solvent phase recombination of CO with HbA is on the order of 2×10^6 M^{-1} s^{-1} for the R-state and about a factor of 50 slower for the T state (*28*). The R and T state solvent processes are much slower than any tertiary relaxation events occurring after photodissociation. In the present study, comparing the different β93-modified Hbs to unmodified HbA, resonance Raman spectra were generated from solutions containing either the equilibrium deoxy forms or the CO saturated forms. For the latter, the spectra generated are of the photoproduct occurring within 10 ns of photodissociation or the CO−heme complex. Ligand rebinding kinetics are compared for solution phase CO saturated samples and for sol−gel encapsulated CO saturated samples.

Sol−gel encapsulated Hb proved to be very useful in identifying conformation-dependent aspects of the ligand-binding kinetics of β93-modified forms. In traditional solution phase studies, one probes the geminate rebinding from the equilibrium form of the liganded species (typically the liganded R structure) and the bimolecular binding to either the equilibrium deoxy species (typically deoxy T structure) or the quasi-stable deoxy R that appears within microsecond of photodissociation of a liganded R form of Hb. In an attempt to compare the ligand reactivity for both the liganded R and T derivatives, a new approach was used in which either the deoxy or CO saturated Hb derivative is encapsulated in a porous sol−gel (*54*−*60*). The encapsulated protein is in contact with the solvent through the water-filled pores of the sol−gel and can, therefore, undergo ligand binding and ligand loss. Although the state of ligation is easily changed for the encapsulated Hb, the sol−gel can be used to "lock in" the initial conformation and, thus, prevent subsequent ligand induced quaternary structure changes. Recent studies (*60*) show that T-state ligand rebinding kinetics can be obtained from samples in which encapsulated deoxyHbA is exposed to CO, resulting in a liganded T-state species. In the present study, a recently described modification (*60*) of the original encapsulation protocol (*61*) is used, since it was shown (*60*) to be far more effective in preventing conformation change after ligand binding or release.

METHODS AND MATERIALS

Preparation of the Sol−*Gel Encapsulated Hbs.* Sol−gel encapsulated samples were prepared using a new preparative protocol described in detail elsewhere (*60*). Briefly, this new protocol differs from the standard preparation derived from proton initiated hydrolysis/condensation reaction of tetramethyl orthosilicate (TMOS) (Aldrich) (*61*) in that all of the solutions added to the TMOS contain 25 vol % glycerol and that a gentle vortexing step replaces the initial sonication step used in traditional preparation. This protocol yields sol−gels that are much more effective in restricting changes in protein conformations than the initially reported protocol (*61*).

The starting materials for the preparation of the sol−gels are all liquids. The sequence of hydrolysis, condensation and polymerization of the TMOS-based solutions yield tough gel samples, which adopt the shape of the container into which the starting materials were added. Shortly after the hydrolysis/condensation reaction is initiated (while the sample is still completely liquid), an aliquot of Hb solution is added and thoroughly mixed with the evolving TMOS. In the present study, Bis-Tris acetate at pH 6.5 with 25% glycerol was used for the preparation of the sol−gels. All samples were prepared either as a thin 1−3 mm layer on a single surface of a standard 10 $\times$ 10 mm optical cuvette and sealed with airtight ribbed septa, through which gases and solutions could be introduced or removed or as a thin layer on the inside surface of a 10 mm diameter NMR tube. The buffer-immersed gels were stored at 4 °C for at least 12 h after preparation prior to carrying out further experiments. The concentration of Hb in the sol−gel was usually in the range of 0.5−0.6 mM in heme.

Two categories of sol−gel encapsulated COHb were prepared. In one case, referred to as [deoxyHb] + CO, the protein is initially encapsulated as deoxyHbA and subsequently exposed to CO after an aging period of at least 12 h (in the presence of a bathing buffer). The second case designated [COHbA] refers to a sample that is initially encapsulated and aged as COHb.

The absorption spectra of the encapsulated Hbs were all very similar to the corresponding solution phase samples. Absorption spectra were recorded before and after each kinetic measurement in order to determine the condition of the sample with respect to degree of oxidation and state of ligation. The absorption measurements revealed that no changes or degradation in the samples occurred over the course of the experiments.

Preparation of Hbs. Five different maleimide modified Hbs were prepared. Figure 1 shows a schematic of the

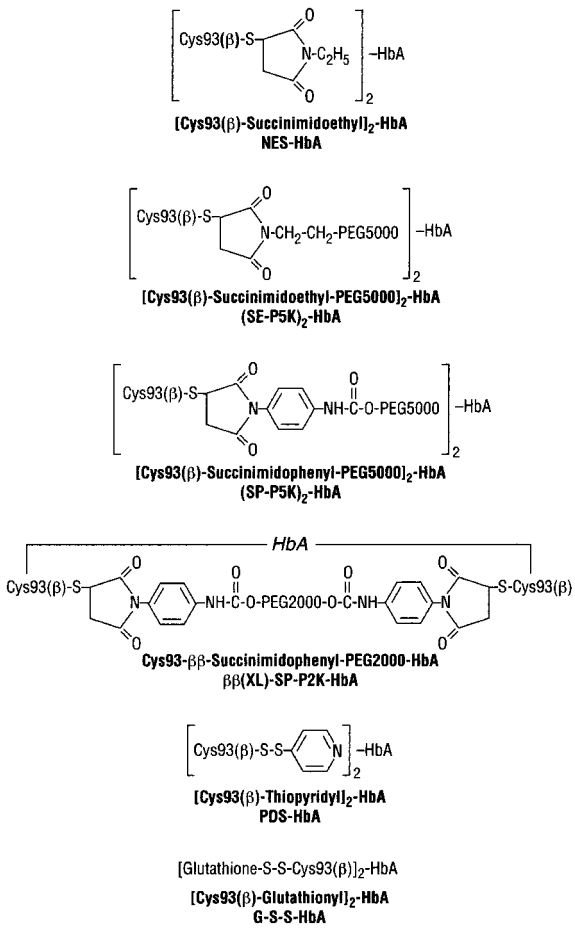

FIGURE 1: A schematic depiction of the different β93 modification reagents.

different β93 modifications used in this study. For two of the materials, NESHbA and NESdes-ArgHbA, *N*-ethylmaleimide (NEM) was used as the reactant. For the other three, the following PEG-linked maleimides were used: Bis-Mal-(maleimide)-Phe-PEG-2000, Mal-Phe-PEG5000, and Mal-Eth-PEG5000 (*O*-(2-maleimidoethyl)-O′ methyl PEG5000). The two modified Hbs having disulfide linkages to β93 were generated using glutathione and 4-PDS(4,4-dithiopyridine) as reactants. The preparative details for all six modified Hbs are described below.

(1) Hemoglobin. HbA was purified from erythrocyte lysate, as described earlier (*62*).

(2) Preparation of Cys-93(β)-Modified HbA. (a) Cys-93-ββ-Succinimidophenyl PEG2000 HbA (ββ-SP-P2K-HbA). ββ-SP-P2K-HbA, a cross-linked derivative containing a single bifunctional PEG2000 chain bridging the two β93 residues, was prepared by reaction of HbA with Bis-Mal (maleimide)-Phe-PEG-2000 in PBS, pH 7.4, followed by ion-exchange chromatography on a CM-Cellulose column, as described by Manjula et al. (*6*).

(b) $(SP-P5K)_2$-HbA and $(SE-P5K)_2$-HbA. HbA was surface decorated at its Cys-93(β) with PEG5000 using two different PEG-maleimide reagents that differ in the spacer linking the reactive maleimide moiety to the PEG moiety (Acharya, unpublished results). $(Succinimidophenyl-PEG5000)_2$-HbA or $(SP-P5K)_2$-HbA was prepared by reaction of HbA with Mal-Phe-PEG5000 (BioAffinity Systems, Rockford, IL). Briefly, HbA (0.5 mM in tetramer) in PBS, pH 7.4, was reacted with 5-fold molar excess of Mal-Phe-PEG5000 for 16−24 h in the cold. The modified protein was separated from the excess reagents by passing the reaction mixture through a Sephadex G25 column. $(Succinimidoethyl-PEG5000)_2$-HbA or $(SE-P5K)_2$-HbA was prepared by reaction of HbA with *O*-(2-maleimidoethyl)-*O′* methyl PEG5000 (Fluka Biochemicals) employing the same procedure as that described above for the preparation of $(SP-P5K)_2$-HbA.

(c) G-S-S-HbA. Glutathionyl HbA was prepared by a two-step process. In the first step, HbA was converted to a mixed disulfide of thiopyridine. HbA (1 mM) in PBS, pH 7.4, was incubated with a 5-fold molar excess of dithiopyridine on ice for 1 h. The thiopyridyl HbA was separated from the excess reagents by gel filtration through a column of Sephadex G25 in PBS, pH 7.4. The thiopyridyl HbA (0.5 mM) was then incubated with a 20-fold molar excess of reduced glutathione at 4 °C overnight and gel filtered on Sephadex G25 again to isolate the glutathione-HbA adduct. Modification of the Cys-93(β) was confirmed by the failure of G-S-S-HbA to react with Mal-Phe-PEG5000, and by the absence of any free thiols in oxy-G-S-S-HbA on titration with 4,4-dithiopyridine by the method of Ampulski et al. (*63*). Isoelectric focusing analysis demonstrated that the product was homogeneous and free of unreacted HbA.

(3) NEM (N-Ethylmaleimide) Treatment. NESHbA was made by treating 3 mL of 0.05 M bis-tris solution 1 mM (heme) HbA_0 with 3 mM NEM achieved by adding 45 μL of 0.2 M NEM (protein:NEM ratio of 1:3). The reaction mixture was incubated at 5 °C for 1 h. The reaction is stopped by dialysis vs 0.05 M hepes at pH 7.4 overnight.

(4) NESdes-ArgHbA. The des-Arg(α141)HbA was prepared using carboxypeptidase B (CPB) digestion. A 1 mL sample of HbA_0 was passed down a Pharmacia type PD-10 column and eluted with 0.05 M tris, pH 8.3. The Hb concentration was approximately 1 mM in heme. An aliquot of 0.5 mL of CPB stock solution (7.6 mg/mL) was then added to 4.4 mL of the eluted Hb solution (77 mg of heme) yielding a 1:200 ratio of protein to enzyme. Prior to the addition of the CPB, 45 μL of 100 mM CPA inhibitor was added to the eluted HbA stock solution yielding a concentration of 1 mM. After the addition of CPB, the sample was converted to the CO form and incubated at 37 °C for 1 h, followed by dialysis vs 0.05 M bis-tris, pH 7.4. The resulting des-ArgHbA was then modified with NEM as described above for the preparation of NESHbA.

(5) 4-PDS (4,4-Dithiodipyridine) Modified HbA. Pyridine disulfide HbA was prepared by reacting HbA with 4-PDS using a previously described protocol (*15*, *63*). The reaction was monitored by following the appearance of one of the products of the reaction, 4-thiopyridone, in the near UV absorption spectrum as previously described (*63*).

All samples used for both kinetic and Raman measurements were at least 0.5 mM in heme. A pH 6.5, Bis-Tris acetate (50 mM) buffer was used both for the solution samples and for the bathing buffer for the sol−gel samples.

Kinetic Measurements. The flash photolysis apparatus employed for the carbon monoxide (CO) rebinding rate experiments is based on pump−probe optical setup described in detail in earlier work (*60*, *64*). The frequency-doubled output of a Nd:YAG laser (5−7 ns, Surelite & Minilite lasers, Continuum) at 532 nm and 2 Hz repetition rate served to photolyze the carbonmonoxy Hb derivatives. Recombination of the CO was monitored by measuring the change in sample

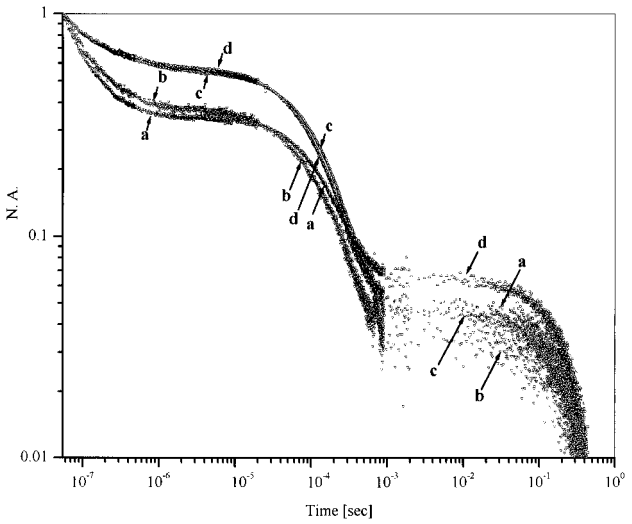

FIGURE 2: Kinetic trace showing the geminate and bimolecular rebinding of carbon monoxide after the 8 ns photodissociation of COHbA (a), PDS-COHbA (b), CONESHbA (c), and $\beta\beta$(XL)-SP-P2K-COHbA (d). Samples (0.5 mM in heme) were all maintained at 3 °C in pH 6.5 50 mM Bis-Tris acetate buffer.

absorption at 441.6 nm (CW, HeCd laser, Liconix). The HeCd probe laser beam was passed through the studied sample (1 mm path-length cuvette for solution phase samples) nearly collinear with the Nd:YAG beam and was separated from the second harmonic generation of Nd:YAG laser of 532 nm using a dichroic mirror. The intensity of the cw blue probe beam was maintained (using a variable attenuator) at a level that produced no noticeable effects on the kinetics and minimal photoproduct population. Absorption spectra and reproducibility of sequential kinetic traces were used to evaluate sample damage. Samples invariably showed no signs of laser induced alterations.

The kinetic traces are displayed on a log−log plot of survival probability or absorbance versus time. Plotting the full kinetic trace for the rebinding of CO to photodissociated COHbA (using a nanosecond photolysis pulse) on a log time axis, allows for a clear separation among the three rebinding processes: geminate rebinding, R-state bimolecular rebinding, and, when applicable, T state bimolecular rebinding. An advantage of a log−log plot is that the kinetics of even a small population of a kinetically distinct species can be observed. Furthermore, on a log−log plot exponential rate constants are easily approximated since exponential traces appear as horizontal lines that abruptly curve down and intersect the time axis at $1/k$, where the k is the rate constant in $\exp(-kt)$.

Visible Resonance Raman Spectroscopy. Visible resonance Raman (VRR) spectra were generated using 8 ns pulse at 435.8 nm. The apparatus and methods for generating, detecting and analyzing the Raman spectra were as previously reported (*46*, *47*, *64*) except that in the present case, a 0.27 m single spectrograph (Spex) with an intensified CCD detector (Princeton Instruments) was used for dispersing and detecting the Raman scattered light.

RESULTS

CO Rebinding Kinetics at pH 6.5 in Solution. Figure 2 shows the 4 °C CO rebinding kinetics at pH 6.5 for (a) HbA, (b) 4-PDS modified HbA, (c) NESHbA, and (d) Cys-93-$\beta\beta$-succinimidophenyl PEG2000 HbA [also referred to as either $\beta\beta$-SP-P2K-HbA or (PEG2000) XLHbA]. Also studied but not shown are the rebinding kinetics for NESdes-ArgHbA, (succinimidophenyl-PEG5000)$_2$-HbA or (SP-P5K)$_2$-HbA, (succinimidoethyl-PEG5000)$_2$-HbA or (SE-P5K)$_2$-HbA, and glutathionylHbA or G-S-SHbA. The kinetic traces can be described as alterations observed in three clear-cut phases. The rebinding occurring prior to several microseconds after photodissociation is due to geminate recombination whereas the two slower phases are derived from bimolecular CO rebinding from the solvent. The faster solvent phase is attributed to rebinding to the R-state structure and the slower phase is derived from rebinding to that fraction of the photoproduct population that has undergone the quaternary switch to the low affinity T structure. At the concentrations of Hb used, there is minimal contribution to the kinetics from $\alpha\beta$ dimers of Hb. In the case of the cross-linked Hb, there is clearly no issue of dimers being present.

Table 1: Geminate Yield (GY) and the Iron-Proximal Histidine Stretching Frequency [ν(Fe-His)] Associated with the Photoproducts of the Carbonmonoxide Derivatives of Both HbA and β93-Modified Forms of HbA at 3 °C in pH 6.5 Bis-Tris Acetate Buffer[a]

Hb species	GY	ν(Fe-His) (cm^{-1})
HbA	0.65	230
HbA + IHP	0.45	226
[COHbA]	0.80	230*
[deoxyHbA] + CO	0.25	222*
NES HbA	0.45	226.0
NESHbA + IHP	0.42	226.0
[CONESHbA]	0.60	nd
[deoxyNESHbA] + CO	0.35	nd
NESdes-ArgHbA	0.42	225.5
NESdes-ArgHbA + IHP	0.40	225.5
[CONESdes-ArgHbA]	0.60	nd
[deoxyNESdes-ArgHbA] + CO	0.55	nd
$\beta\beta$(XL)-SP-P2K-HbA	0.42	226.5
$\beta\beta$(XL)-SP-P2K-HbA + IHP	0.38	226.0
$\beta\beta$(XL)-SP-P2K-HbA + IHP + L35	nd	225.0
(SP-P5K)$_2$-HbA	0.42	226.5
(SP-P5K)$_2$−HbA + IHP	0.40	226.0
(SE-P5K)$_2$-HbA	0.42	227.0
(SE-P5K)$_2$-HbA + IHP	nd	nd
G-S-S-HbA	0.60	229.0
G-S-S-HbA + IHP	0.55	228.0
PDS HbA	0.62	nd

[a] The designation nd indicates that the measurement was not determined. The Raman frequencies for ν(Fe−His) have been approximated to the nearest half wavenumber. The bracketed species refer to sol−gel encapsulated samples (see text for details). The Raman frequencies designated (*) refer to as results from Peterson, Samuni, and Friedman that are to be described in detail in a future publication.

All of the β93 modified Hbs show a reduction in the geminate yield (the percentage of the photoproduct population undergoing geminate recombination) compared to unmodified HbA (see Table 1). Whereas, both nonmaleimide based modifications (PDS and glutathione) show only a small decrease in the geminate yield of a few percent, all five of the maleimide-based derivatives show essentially the same substantial ∼23% decrease (from ∼65% to ∼42%). The same decrease is seen for both PEG(5000)$_2$ modified derivatives despite the difference in the linker group between the maleimide and the start of the PEG chain (phenoxy versus ethoxy). The same kinetic pattern observed at pH 6.5 holds for samples studied at pH 7.5 in Bis-Tris acetate. All of the

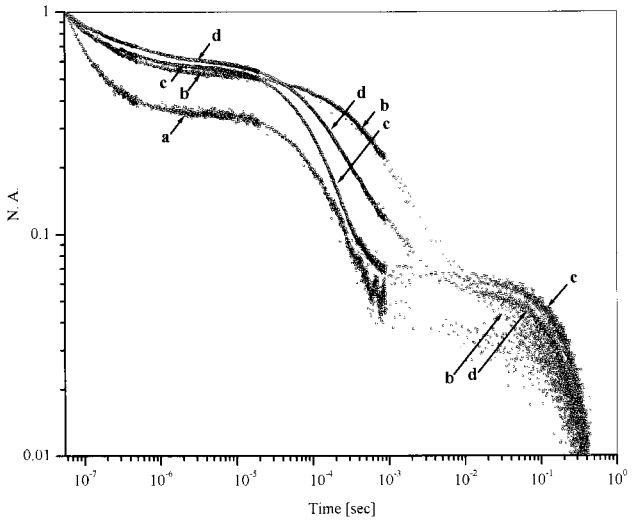

FIGURE 3: Kinetic trace showing the geminate and bimolecular rebinding of carbon monoxide after the 7 ns photodissociation of the CO liganded derivatives of HbA (a), HbA + IHP (6× excess over Hb tetramer concentration) (b), ββ(XL)-SP-P2K-HbA (c), and ββ(XL)-SP-P2K-HbA + IHP (6× excess over Hb tetramer concentration) (d). Samples (0.5 mM in heme) were all maintained at 3 °C in pH 6.5 50 mM Bis-Tris acetate buffer.

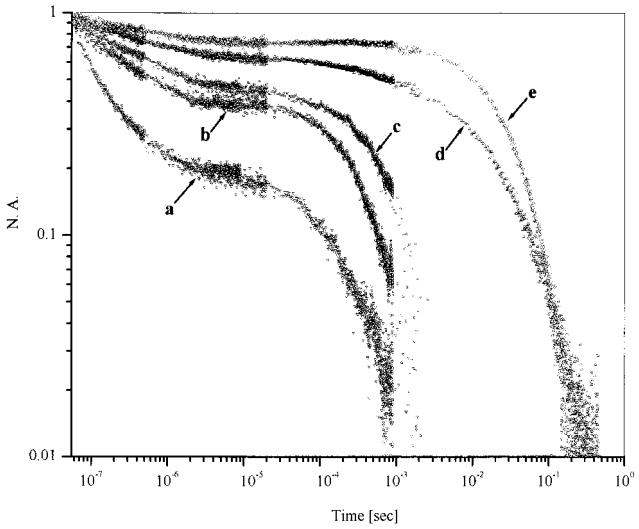

FIGURE 4: Kinetic trace showing the geminate and bimolecular rebinding of carbon monoxide after the 8 ns photodissociation of sol−gel encapsulated Hbs: [COHbA] (a), [CONESdes-ArgHbA] (b), [deoxyNESdes-ArgHbA] + CO (c), [deoxyNESHbA] + CO (d), and [deoxyHbA] + CO (e). The brackets indicate the initial species encapsulated in the porous sol−gel. The + CO designation refers to CO added after the [deoxyHb] sol−gel sample has aged at least overnight. Samples (final concentration of Hb in the sol−gel was approximately 0.5 mM in heme) were all maintained at 3 °C in a pH 6.5 Bis-Tris acetate buffer.

samples show very similar kinetics associated with the fast (R-state) bimolecular solvent phase rebinding. Under the conditions used to make the current kinetic measurements, the T-state kinetics constitute only a very small fraction of the total rebinding and, as a consequence, they are hard to characterize and compare. A future study will focus on the slower kinetic phases.

Effect of IHP on the CO Rebinding Kinetics of β93 Modified HbA in Solution. A representative comparison with HbA of the IHP effect on the CO rebinding kinetics of β93 modified HbA at pH 6.5 is shown in Figure 3. The kinetics observed for the ββ(XL)-SP-P2K-COHbA and COHbA are shown in the figure. It can be seen that for the PEG modified sample, there is a small IHP induced decrease in the geminate yield and a slowing of the R-state bimolecular kinetics. Similar results were obtained for all of the β93 modified derivatives (see Table 1). The same pattern of IHP induced changes in the geminate yield and the rate of the R-state bimolecular rate was observed at pH 7.5; however, at pH 7.5, the IHP-induced reduction in the GY of all the Hbs was less than at pH 6.5. It can be seen that the pattern observed for the β93 modified samples holds for COHbA in that IHP reduces the geminate yield and slows the R-state bimolecular kinetics; however, compared to what occurs in the β93 modified Hbs, the IHP effect in HbA is clearly much larger both in terms of a fractional reduction in the GY and the degree of slowing for R-state bimolecular rebinding.

CO Rebinding Kinetics of HbA, NESHbA, and NESdes-Arg HbA Encapsulated in a sol−gel Matrix. Figure 4 shows the CO rebinding kinetics for HbA, NESHbA, and NESdesArgHbA encapsulated in a porous sol−gel. As described in the Materials and Methods, the encapsulated derivatives were prepared using two different protocols. In one case, [deoxyHb] + CO, the deoxy derivative is first encapsulated and after a period of aging the sample is exposed to CO. The other class of sample, [COHb], is generated by encapsulating the CO saturated derivative from the start.

Figure 4 shows the kinetics from (a) [COHbA], (b) [CONESdes-ArgHbA], (c) [deoxyNESdes-ArgHbA] + CO, (d) [deoxyNESHbA] + CO, and (e) [deoxyHbA] + CO. Also studied but not shown are the kinetics from [CONESHbA] which are very similar to those shown for [CONESdes-ArgHbA]. For all of [COHb] samples, there is a single bimolecular kinetic phase which is very similar to the fast phase observed for the solution phase samples under similar conditions. The GYs for [CONESHbA] and [CONESdes-ArgHbA] are similar (∼60%). This value is lower than the GY of 80% for [COHbA] (see Table 1).

The traces c−e are derived from samples initially encapsulated in their respective equilibrium deoxy state, i.e., [deoxyHb] + CO. Whereas the traces for [CONESHbA] and [CONESdesArgHbA] are very similar, the traces derived from their respective encapsulated deoxy forms are not. The [deoxyNESdes-ArgHb] + CO sample shows both a much larger GY (∼55%) and a bimolecular recombination phase that is only slightly slower than what is observed for both the corresponding [CONESdes-ArgHbA] sample and the [COHbA] and [CONESHbA] samples. The [deoxyNESHbA] + CO and the [deoxyHbA] + CO samples both exhibit a much reduced GY compared to the corresponding encapsulated CO derivative (see Table 1) and a bimolecular recombination phase that is similar to the slowest phase observed in solution after photodissociation of the CO derivative. It can be seen that the GY for the [deoxyNESHbA] + CO sample is slightly greater than that from the [deoxyHbA] + CO sample. The inclusion of IHP with the deoxyHb solutions when initially encapsulating the deoxy samples results in a further reduction of the GY for both [deoxyNESHbA] + CO and the [deoxyHbA] + CO samples.

Visible Resonance Raman Spectra of β93 Modified HbA. Figure 5 shows the ν(Fe-His), the iron-proximal histidine stretching band in the 435.8 nm generated resonance Raman

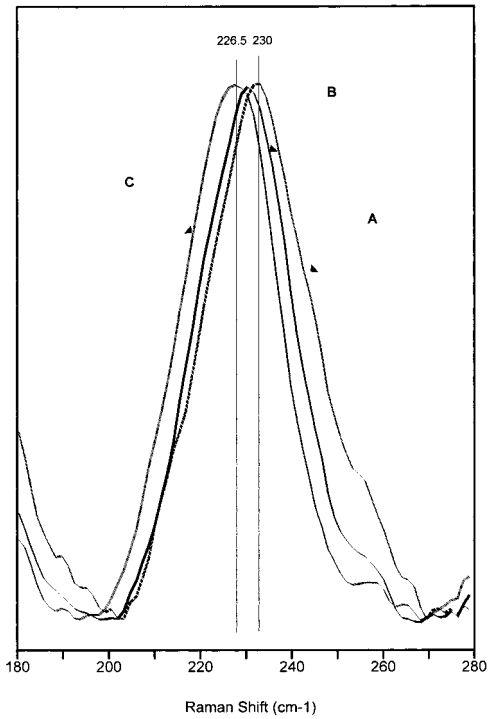

FIGURE 5: A segment of the low-frequency resonance Raman spectrum showing ν(Fe-His), the iron-proximal histidine stretching mode generated from the 8 ns photoproduct of the CO saturated derivatives of: HbA (a), G-S-S-HbA (b), and $(SP\text{-}P5K)_2$-HbA (c). Samples (0.5 mM in heme) were all maintained at 3−7 °C in pH 6.5 50 mM Bis-Tris acetate buffer.

spectra of the 8 ns photoproduct generated from the CO derivative of both HbA and two β93 modified HbAs (see Table 1). The shown spectra and peak positions from $\beta\beta$-(XL)-SP-P2K-COHbA and $(SP\text{-}P5K)_2$-COHbA are typical of all of the derivatives generated via maleimide reactions. With respect to COHbA, all of the maleimide modified derivatives show a similar decrease of $\sim$4 cm^{-1} in the frequency ν(Fe-His). The photoproduct derived from the G-S-S-COHbA sample showed a much smaller shift of $\sim$1 cm^{-1} (mainly in the form of broadening on the low-frequency side of the band). The addition of IHP to the CO maleimide derivatives resulted in very small decreases of $\leq$1.5 cm^{-1} in the frequency of ν(Fe-His) in the photoproduct spectra. A small IHP induced decrease in frequency of about 1 cm^{-1} was observed for G-S-S-COHbA. In contrast, and as previously reported (*38*, *39*, *46*), the addition of IHP to COHbA results in a decrease in the frequency of ν(Fe-His) of $\sim$4 cm^{-1} for the 8 ns photoproduct.

With the exception of NESdes-ArgHbA, the resonance Raman spectra of the deoxy derivatives for the β93 modified Hbs and for HbA are all very similar. Previously reported results (*65*) demonstrated that NEMdes-ArgHbA shows a large increase of 6 cm^{-1} in the frequency of ν(Fe-His) relative to the value observed for deoxyHbA ($\sim$215 cm^{-1}). The other β93 deoxy derivatives exhibit a ν(Fe-His) band having frequencies much closer to that of unmodified deoxyHbA. The broadness of the ν(Fe-His) band for the deoxy derivatives makes accurate peak positions difficult; however, the frequency of the ν(Fe-His) band for several of the β93 derivatives appear to be between 1 and 2 cm^{-1} higher than for HbA. The addition of IHP has little effect on the deoxyHbA spectrum, as previously reported, but shifts the modified forms so that in the presence of IHP all but the NESdes-Arg derivatives have virtually the same frequency for ν(Fe-His) as deoxyHbA. Even in the presence of IHP, the deoxyNESdes-Arg derivative has a peak that is 3 cm^{-1} higher in frequency than deoxy HbA as reported in earlier studies (*65*).

DISCUSSION

Sol−Gel Encapsulated Hbs: A Method for Restricting Conformational Change. Encapsulation of proteins in porous sol−gels is an approach for generating Hb intermediates that are not accessible through conventional time-resolved techniques such as flash photolysis and rapid mix. It has been shown that many proteins can be encapsulated in porous sol−gels derived from tetramethyl orthosilicate (TMOS) with a retention of functionality and enhanced stability (*61*, *64*, *66*, *67*). The sol−gel matrix traps the protein, but both solvent and small solute molecules can diffuse into the sol−gel through a network of 50−100 Å diameter pores. These small molecules can bind to or react with the encapsulated protein molecules. Thus, oxyHbA can be encapsulated, but the oxygen can still be removed by the addition of sodium dithionite. Similarly, encapsulted deoxygenated HbA (deoxyHbA) can become saturated with ligands (O_2, CO, or NO) when ligand is introduced into the solvent bathing the gel.

Pioneering measurements of oxygen binding and dissociation curves derived from encapsulated deoxy and oxyHbA at 10 °C indicated an absence of cooperative ligand binding (*54*, *55*). The encapsulated deoxyHbA was shown to bind and release oxygen with low affinity, consistent with the properties of a noncooperative T state species. In contrast, encapsulated O_2HbA was shown to lose and rebind oxygen with high affinity, in a manner consistent with a trapped R-state species. These and subsequent studies (*56*, *57*, *60*) strongly suggested that the sol−gel greatly slows the ligation associated relaxation of the quaternary structure of the initially encapsulated population. Thus, when deoxyHbA and O_2HbA are encapsulated, there is an extended period of time during which the T and R structures are maintained respectively even when the ligation status of the heme is changed.

The altered oxygen binding properties reported for sol−gel encapsulated Hb raised the exciting prospect of using sol−gels to trap nonequilibrium species, such as liganded T and deoxy R. A full analysis of the potential of this technique required a more detailed probe of the functional, conformational, and dynamical behavior of the encapsulated proteins. Resonance Raman spectroscopy was used to help determine the extent to which both tertiary and quaternary conformational changes are restricted in the sol−gel. Visible resonance Raman spectra of a deoxygenated sample of encapsulated HbA generated by adding dithionite to an encapsulated O_2-HbA sample revealed that both tertiary and quaternary structural changes are slowed as the sol−gel is cooled (*58*). A UV resonance Raman study (*59*) on encapsulated deoxyHbA exposed to CO revealed that at 4 °C the addition of CO minimally perturbs the quaternary or tertiary structure of the encapsulated T state HbA. Subsequent spectra, obtained after allowing the sample to remain at ambient temperatures for a few hours, indicated additional conformational changes reflecting T→R changes in the hinge region

but not the switch region of the T−R sensitive $\alpha_1\beta_2$ (and $\alpha_2\beta_1$) interface. These two Raman studies clearly showed that sol−gel encapsulation is a viable method for overcoming the diffusion and mixing time limitations in a typical rapid mix experiment. In a more recent study (*60*), it was shown that sol−gel encapsulated Hbs can yield high quality ligand rebinding kinetics after nanosecond photodissociation and that a modification of the original sol−gel preparative protocol is considerably more effective in restricting the conformational relaxation of the initially encapsulated structures after the addition or removal of ligands. This newer protocol was used in the present study to trap the conformations of the initially encapsulated derivatives of β93 modified HbA.

Geminate Recombination for R-State Solution Phase Species. Several studies indicate that the geminate yield for Hbs is highly responsive to quaternary structure (*38*−*45*). In general, the geminate yield appears to decrease significantly in going from an R-state to T state form of a given Hb. Using iron-metal hybrids (*42*), double pulse excitations (*40*), mixed ligation states (*44*), and allosteric effectors (*43*), it was inferred that the geminate yield for T state COHbA is just a few percent. In contrast, the geminate yield for R-state COHbA is approximately 50% at 25 °C (*32*−*34*, *36*). Through the use of sol−gel encapsulation techniques, it was directly demonstrated that the geminate phase for T state COHbA is only a few percent (*60*) as predicted from the above earlier indirect studies. The geminate yield has also been shown to decrease for R-state liganded HbA when allosteric effectors are added (*37*, *38*, *47*). These results suggest that tertiary structure changes within the R-state in the direction of the T state also decrease the geminate yield. Relaxation of tertiary structure within the R-state after photodissociation is claimed to progressively increase the kinetic barrier for geminate recombination (*39*, *45*, *49*). It follows that a slow-down in the tertiary relaxation due to either viscosity effects (*68*, *69*) or mutations (*47*) can result in an enhanced geminate yield. A comparable effect for the T state has also been proposed (*49*, *70*). As with the R-state, the T state should manifest at least two tertiary conformations: the deoxy T and liganded T structures. The more R-like liganded T conformations should exhibit a higher geminate yield than those closer to the extreme deoxy T conformation. As a consequence, the rate of relaxation of the liganded T conformation toward the deoxy T conformation after photodissociation should also play a role in determining the geminate yield for T state liganded species.

In the absence of added allosteric effectors, all of the Hbs in the present study are expected to adopt the R quaternary structure when fully liganded. Indeed the maleimide modification of β93 has been shown to favor the R quaternary state (*16*−*18*, *22*−*25*). The doubly modified NESdes-ArgHbA has been shown to be minimally cooperative in that the deoxy derivative can be readily stabilized in the R-state (*22*). The observation in the present study that all of the effector-free samples exhibit a typical R-state bimolecular recombination process with approximately the same rate is consistent with the population of CO saturated derivatives being overwhelmingly R-state.

As anticipated (vide supra), we find that, in general, the addition of allosteric effectors reduces the geminate yield. Unexpectedly, the degree of reduction in the geminate yield brought about by IHP is greatly reduced for β93 modified derivatives. Even more surprising is the large reduction in the geminate yield for COHbA when derivatized with maleimide. The effect is clearly maleimide specific since virtually the same reduction in geminate yield occurs for the wide variety of maleimide modified forms examined but not for the nonmaleimide β93 modified Hbs. Thus, the maleimide induced modification of COHbA results in both a reduction in the geminate yield and a diminished response of the geminate rebinding to the addition of IHP. Earlier studies (*22*−*25*) have shown that the reactivity of NESHbA toward dioxygen is reduced relative to HbA as reflected in K_4 differences. The present study indicates that at least part of this reduction in reactivity is kinetic in origin.

The reduction in geminate yield for R-state species either through the maleimide modification of β93 or the addition of allosteric effector can originate either through an alteration of the tertiary structure within the R quaternary state that impacts the ligand binding site or an enhancement of the sub-microsecond relaxation of the local tertiary structure upon photodissociation of the COHb. Monitoring the geminate rebinding for sol−gel encapsulated samples helps to discriminate between the two mechanisms since at 4 °C tertiary relaxation on the sub-microsecond time scale is greatly slowed (*58*). Furthermore, by virtue of preventing interconversion of distinct conformational populations, the encapsulation protocol can establish if there are multiple populations of functionally distinct species present in the equilibrium distribution (e.g., the presence of both R and T state forms of the CO derivative). The presence of distinct high and low affinity populations trapped in the sol−gel would result in the presence of distinct and separable kinetic traces for the bimolecular solvent phase rebinding. An analysis of the sol−gel results with respect to this issue is discussed below.

R-State Geminate Recombination for sol−gel Encapsulated Derivatives. The geminate recombination for the sol−gel encapsulated CO derivatives of HbA, NESHbA, and NESdes-ArgHbA shows two distinct features (1) the geminate yield is enhanced over that derived from the corresponding solution phase and (2) the reduced geminate yield observed for the maleimide-modified samples is maintained in the sol−gel.

The enhancement in the geminate yield for all of the encapsulated samples is explainable in terms of a combination of two effects: (i) an extended geminate phase due to an increase in viscosity resulting in a slow in the rate of ligand escape from the protein to the solvent and (2) a slow or cessation in tertiary relaxation occurring on the same time scale as geminate recombination. A slow of tertiary relaxation would have the effect of lowering the effective potential energy barrier controlling the binding of the CO to the heme (*47*, *49*, *69*, *71*). The observation that, under these conditions of slowed tertiary relaxation, the reduction of the geminate yield for the maleimide derivatives is fully maintained, argues that this reduction arises at least partially from differences in the R structure of the initial liganded species. Furthermore, the appearance of only a single phase for the bimolecular rebinding kinetics indicates that the reduced geminate yield is not the result of there being a mixed population consisting of both an R-state population similar to that associated with COHbA and a lower affinity population having a reduced geminate yield.

Effector-Induced Changes in the Liganded R-State. The solution results presented show that IHP reduces the R-state geminate yield and slows the rate of the R-state bimolecular recombination as has been shown in earlier studies (*43*). The effect is maximal for HbA and minimal for the β93 derivatives of HbA. That the addition of IHP impacts the Raman spectrum of the 8 ns photoproduct of COHbA indicates that the effect is likely to originate at least in part from a static alteration of the liganded R-state conformation. That conclusion is also consistent with observations of IHP-induced spectroscopic changes observed for the liganded species (*72*). Furthermore, that conclusion is consistent with the earlier claim (*43*) that liganded HbA in the presence of effectors adopts an R-state tertiary conformation that is functionally distinct from that of the effector free population.

Effector Modified R-State and β-93 Modified R-State: A Functional Comparison. The geminate yield for COHbA is reduced both upon addition of allosteric effectors and upon maleimide modification of β93. The similar pattern of reduction in the geminate yield raises the possibility that both alterations produce the same modified liganded R-state conformation. A comparison of the R-state bimolecular recombination in solution reveals that whereas the allosteric effectors reduce the geminate yield and slow the bimolecular rate, maleimide modifications only bring about the former. This difference argues in favor of distinctly different pathways through which each of these modifications impacts the R-state. It is also clear that modification of β93 interferes with the mechanism through which IHP reduces the rate of the R-state bimolecular recombination. This conclusion follows from the observation that addition of effectors to the β93 derivatives does not produce the same degree of slowing of the bimolecular rebinding as is observed for HbA. An earlier study using a fluorescent analogue of DPG (*73*) showed that at pH values comparable to those used in the present study, the CO derivative of $(PEG2000)_2$XLHbA binds the DPG analogue even more effectively than COHbA. It follows that maleimide induced alteration of β93 does not interfere with effector binding to the R-state (it may even enhance it), but does to some extent disrupt the communication pathway through which effector binding impacts R-state reactivity as reflected in the geminate and bimolecular rebinding processes. A recent X-ray crystallographic study of a chemically modified HbA (*74*), in which the DPG binding site is modified through a cross-link between the two β82 lysines, reveals possible communication pathways between the DPG binding site and both β93 and key surrounding residues such as Tyr β145.

Correlation of Geminate Yield with ν(Fe−His). In the absence of distal heme pocket alterations, the frequency of ν(Fe-His) for the photoproduct at 8 ns derived from the various carbonmonoxy Hbs usually correlates with the geminate yield (*39*, *41*, *45*, *46*). The geminate yield is observed to decrease for those species that have the lower frequency. The correlation clearly extends to the present study where the geminate yield and the frequency of ν(Fe-His) for the photoproduct both decrease in the following sequence: COHbA; nonmaleimide modified COHbAs; maleimide modified COHbAs. Similarly in those cases where the addition of IHP lowers ν(Fe-His), the geminate yield also decreases, with the decrease scaling with the magnitude of the frequency reduction of ν(Fe-His).

To extend the correlation to the deoxy samples requires generating the frequency of ν(Fe-His) for the photoproduct of samples prepared as [deoxyHb] + CO. Under these conditions, the spectra reflect both the quaternary structure of the initially encapsulated deoxy derivative and the tertiary structure changes within the sol−gel (to the extent that they occur) resulting from ligand binding within that quaternary state. Such studies are currently in progress. In the present study, the comparison of the CO rebinding kinetics for [deoxyNESdes-ArgHbA] + CO, [deoxyNESHbA] + CO and [deoxyHbA] + CO correlate with the frequency of ν(Fe-His) of the solution-phase deoxy derivatives. The latter two both exhibit deoxy T state values for the frequency of ν-(Fe-His) and T state kinetics. The [deoxyNESdes-ArgHbA] + CO sample exhibits R-state kinetics and the corresponding deoxy derivative yields an R-state frequency for ν(Fe-His) (*65*). The difference in both the geminate and bimolecular CO rebinding kinetics between [CONESdes-ArgHbA] and [deoxyNESdes-ArgHbA] +CO are likely to reflect differences in the R-state tertiary structures that originate from the sol−gel limiting tertiary relaxation both upon ligand photodissociation and ligand binding, respectively.

The correlation between the geminate yield and the frequency of ν(Fe-His) can be explained in terms of both proximal constraint and proximal enhancement. In five coordinate ferrous Hbs, the heme-iron is several tenths of an angstrom out of the heme-plane. The formation of a stable CO bound ferrous derivative requires that the iron move into the heme-plane. The movement of the iron also entails movement of the proximal imidazole (from His F8) and the F helix to which this imidazole is attached. The molecular work required to move the "protein-decorated" iron upon CO ligation contributes to the potential energy barrier controlling the formation of the six coordinate CO-heme species in Hb (*39*, *45*, *75*, *76*). Proximal strain is a term that refers to the added work required to move the iron in plane under conditions where the tertiary/quaternary structure counters that motion. Such is the case for the typical T state Hbs where at least for the α subunits, the protein constrains the proximal imidazole to a tilted orientation that energetically favors an out-of-plane iron configuration for the heme. The frequency of ν(Fe-His) is a good indicator of conformations that functionally manifest proximal strain (*39*, *41*, *45*, *46*). Raman studies on both protein and model porphyrin samples indicate that frequencies for ν(Fe-His) in the range of 220−224 cm^{-1} reflect an unconstrained proximal environment. The dramatically lower frequencies (<210 cm^{-1}) observed for the α subunits of T state deoxy Hbs are reflective of a conformation that exhibits proximal strain when undergoing ligand binding.

Proximal enhancement (*47*) is a term that refers to a reduction in the energy cost of moving the iron in plane upon ligand binding that arises from the protein constraining the F helix to a "hyper-favorable" conformation with respect to ligand binding. Such a situation has been proposed for the photoproduct of R-state COHbA (*47*). Upon photodissociation of the CO, the iron moves out of the heme plane within at most a few picosecond (*76*−*78*). The ability of the proximal imidazole to follow that motion depends to a large measure on the "vertical" mobility of the F helix. If the F helix is slow to accommodate the movement of the iron and proximal imidazole, there will be an extended period during

which there is a compressed Fe−His bond (*79*). The compressed bond is reflected in an increase in the frequency of ν(Fe-His) as observed in the photoproduct of COHbA (*79*−*81*). In this picture, the nanosecond to microsecond relaxation of ν(Fe-His) for photodissociated R-state COHbA is reflective of a decompression of Fe−His bond as the F helix undergoes tertiary relaxation from the liganded R conformation to that of the deoxy R conformation. It has been proposed (*52*) that this relaxation takes the form of "clam shell" type rotation of the F and E helices. Ligand rebinding to the "relaxed" deoxy R conformation requires that the iron, the proximal imidazole and the F helix all shift; whereas, ligand rebinding to the unrelaxed photoproduct does not require the movement of the F helix. As a result, the energy cost for ligand rebinding is lower for the unrelaxed photoproduct. This effect has been proposed (*47*) to be the conformational origin of quaternary enhancement. Quaternary enhancement is the increase in ligand binding reactivity of the R-state tetramer over that of the dissociated dimers (*19*−*21*). Within the above model, the loss of the quaternary enhancement for a modified or mutant liganded HbA would be reflected both in a reduced frequency for ν(Fe-His) from the 8 ns photoproduct and a reduction in the geminate yield. All of the maleimide-modified HbAs in the present study fulfill those criteria for a reduction of the quaternary enhancement effect.

Conformational Origins for Altered Functional Properties Associated with β 93 Modified deoxyHbA. Studies (*23*−*25*) have shown that NEM modified derivatives of HbA typically bind the first oxygen with higher affinity (K_1) than does HbA. Whereas, K_1 for NESHbA is only a little more than a factor of 2 greater for HbA, for the NESdes-Arg derivative it attains values associated with a noncooperative R-state (*22*). Several biophysical studies (*65*, *82*−*84*) indicate that the NESdes-Arg derivative of HbA exhibits R-state properties even in the deoxy form. These findings are consistent with the present results that show R-like bimolecular CO rebinding kinetics from photodissociated [deoxy NESdes-Arg HbA] + CO. Thus, all the results indicate that the high K_1 value for NESdes-ArgHbA stems from the full relaxation of T state constraints as reflected at least in part by the 6 cm^{-1} increase in the frequency of ν(Fe-His) (*65*) and 2 nm red shift of absorption Band III (758→760 nm) (*17*) for the deoxy derivative of NESdes-Arg.

Whereas the increase in K_1 for NESdes-ArgHbA can readily be explained in terms of an R-state deoxy derivative, the functional properties of HbA modified exclusively at β93 cannot. Tritium exchange studies (*83*, *84*) show that in solution with respect to destabilization of the T structure, the NES modification of deoxyHbA has a nearly identical energy consequence as loss of His β146 in the desHis derivative of deoxyHbA. Despite the destabilization of the T-state due to the loss of both the Asp β94−His β146 and the His β146−Lys α40 hydrogen bonds, the deoxy derivatives of both species retain the T state conformation. Furthermore, X-ray crystallography reveals that both deoxy desHisHbA (*85*) and deoxy $(PEG2000)_2$XLHbA (*6*) exhibit T state conformations with only very modest local changes around the C-terminus of the β chains.

Despite the clear indications that deoxy derivatives of maleimide modified HbA (with the exception of NESdes-ArgHbA) are stabilized in the T structure, functional studies reveal that K_1 is increased for NESHbA (*23*−*25*) comparable to what is observed for des-HisHbA. Whereas it is readily understandable how the disruption of the Asp β94−His β146 and the His β146−Lys α40 hydrogen bonds results in a destabilization of the T quaternary structure with respect to the R structure, it is not clear how these modification result in the increase in ligand binding reactivity within the T state. The slight increase in the frequency of ν(Fe-His) reflects a communication pathway that ultimately impacts the ligand binding site. An alteration in the interaction between the penultimate tyrosine β Tyr145 and β Val98 is a possible pathway for impacting the β heme-histidine interaction. The tritium exchange studies (*83*, *84*) reveal that the NES modification gets communicated to the N terminus of the α subunits as well. Similarly, Fe−Ni hybrid NESHbA shows that the enhanced ligand binding reactivity extends to both subunits (*26*, *27*). The pathway(s) through which modification of β93 communicates with the α hemes is unclear but might involve the $\alpha_1\beta_2$ interface via a perturbed β99−α42 interaction. The slight increase in ν(Fe-His) observed for the β93 modified deoxy derivatives might represent a decrease in the kinetic barrier for the ligand on rate and hence explain part of the enhanced reactivity. More likely, but as yet unexplored, is the possibility that the global changes observed for β93 modified deoxy derivatives described above influence the stability and perhaps conformation of the liganded T state, which would influence the T state off rates (and T state geminate yield).

Conformational Origins for Altered Functional Properties Associated with β 93 Modified COHb. Isolated β chains (*22*) as well as the intact R-state tetramer show alterations in reactivity upon formation of the NES derivative. The present study indicates that the maleimide modification in particular produces an alteration in conformation of the liganded derivative that is manifested in the substantially reduced frequency of ν(Fe-His) for the 8 ns photoproduct. Within the context of the "clam shell" type of relaxation described above, the maleimide modified derivatives of COHbA could be said to display an F helix that is at least partially relaxed from the energetically more favorable (with respect to rebinding) compressed configuration (vide supra) of the normal COHbA photoproduct to the less favorable configuration of the deoxy R conformation. The present results suggest that the scaffolding (*47*, *86*−*88*) that maintains or stabilizes the F helix in the position that results in the compressed Fe−His bond has been compromised in the maleimide-modified COHb derivatives. Since the β94−β146 and β146−α40 hydrogen bonds are already lost in the R-state structure, the above effect is not likely to originate from those interactions. A more likely origin is from Tyr β145. A crystallographic study of a SNO β93 modified R-state Hb reveals a marked shift in the position of Tyr β145 (89). A disruption of the Tyr β145−Val β98 hydrogen bond is likely to have an impact on the scaffolding supporting the F helix and may therefore be the source of altered R-state properties of maleimide-modified HbA. Furthermore in a previous study, it was proposed that a mutation-induced alteration in the conformation of the Tyr β145 is the source of an enhanced H−F helix scaffolding and an exaggerated quaternary enhancement effect observed in HbYpsilanti-(β99Asp→Tyr) (*47*).

CONCLUSIONS

The present study shows that the conformational and functional consequences to HbA upon modification of β93 are chemistry specific. All of the maleimide-based modifications result in alterations of the liganded (carbonmonoxy) R-state as manifested by a substantial reduction in the geminate yield and a several wavenumber (cm^{-1}) decrease in the iron-proximal histidine stretching frequency for the photoproduct. The disulfide-based modifications result in similar consequences, but with the changes being much smaller. Both classes of modifications are shown to interfere with the full expression of the IHP effect within the liganded R structure. Sol−gel encapsulation is demonstrated to be an effective method for restricting conformational changes that allows for a comparison of kinetics of CO rebinding by the deoxy and liganded conformations of the different β93 modified Hbs.

REFERENCES

1. Dickerson, R. E., and Geis, I. (1983) *Hemoglobin Structure, Function, Evolution, and Pathology*, Benjamin/Cummings, Menlo Park, CA.
2. Jia, L., Bonaventura, C., Bonaventura, J., and Stemler, J. S. (1996) S-nitrosohaemoglobin: A dynamic activity of blood in vascular control. *Nature 380*, 221−226.
3. Stemler, J. S., Jia, L., Eu, J. P., McMahon, T. J., Demchenko, I. T., Bonaventura, J., Genert, K., and Piantadosi, C. A. (1997) Blood flow regulation by S-Nitrosohemoglobin in the physiological oxygen gradient. *Science 276*, 2034−2037.
4. Balagopalakrishna, C., Abugo, O. O., Hoesky, J., Manoharan, P. T., Nagababu, E., and Rifkind, J. M. (1998) Superoxide produced in the hemepocket of the β chain of hemoglobin reacts with β 93 cysteine to produce a thiyl radical. *Biochemistry 37*, 13194−13202.
5. Taboy, C. H., Bonaventura, C., and Crumbliss, A. L. (1999) *Spectroelecrochemistry of hemoglobin and hemoglobin mutants in the presence of allosteric and thiosteric effectors* Am. Chem. Soc. Meeting, Anaheim, CA.
6. Manjula, B. N., Malavalli, A., Smith, P. K., Chan, N.-L., Arnone, A., Friedman, J. M., and Acharya, A. S. (2000) Cys-93-$\beta\beta$-succinimidophenyl polyehtylene glycol 2000 hemoglobin A. *J. Biol. Chem. 275*, 5527−5534.
7. Garel, M.-C, Domenget, C., Galacteros, F., and Beuzard, Y (1984) Inhibition of erythrocyte sickling by thiol reagents. *Mol. Pharm. 26*, 559−565.
8. Craescu, C. T., Poyart, C., Schaeffer, C., Garel, M.-C, Kister, J., and Beuzard, Y. (1986) Covalent binding of glutathione to hemoglobin. *J. Biol. Chem. 31*, 14710−14716.
9. Perutz, M. F., G. Fermi, B., Luisi, B., Shaanan, and Liddington, R. C. (1987). Stereochemistry of cooperative mechanisms in hemoglobin. *Acc. Chem. Res. 20*, 309−321.
10. Perutz, M. F. (1970) Stereochemistry of cooperative effects in Haemoglobin. *Nature (London) 228*, 726−739.
11. Perutz, M. F. (1989) Mechanisms of cooperativity and allosteric regulation in proteins. *Q. Rev. Biophys. 22*, 139−236.
12. Perutz, M. F., Wilkinson, A. J., Paoli, M., and Dodson, G. G. (1998) The stereochemical mechanism of the cooperative effects in hemoglobin revisited. *Annu. Rev. Biomol. Struct. 27*, 1-34.
13. Riggs, A. F. (1961) The binding of N-ethylmaleimide by human hemoglobin and its effect upon the oxygen equilibrium. *J. Biol. Chem. 236*, 1948−1954.
14. Guidotti, G. (1965) The rates of reaction of the sulfydryl groups of human hemoglobin. *J. Biol. Chem. 240*, 3924−27.
15. Taketa, F., and Morell, S. A. (1969) Changes in the 4-PDS reactive SH groups of hemoglobin associated with the binding of phosphates and ligands. *Anal. Biochem. 32*, 170−174.
16. Perutz, M. F., Fersht, A. R., Simon, S. R., and Roberts, G. C. K. (1974) *Biochemistry 13*, 2174−2186.
17. Perutz, M. F., Ladner, J. E., Simon, S. R., and Ho, C. (1974) Influence of globin structure on the state of the heme. I. Human deoxyhemoglobin. *Biochemistry 13*, 2163−2173.
18. Vasquez, G. B., Karavitis, M., Ji, X., Pechik, I., Brinigar, W. S., Gilliland, G. L., and Fronticelli, C. (1999) Cysteines β93 and β112 as probes of conformational and functional events at the human hemoglobin subunit interfaces. *Biophys. J. 76*, 88−97.
19. Doyle, M. L., Lew, G., Turner, G. L., Rucknagel, D., and Ackers, G. K. (1992) Regulation of oxygen affinity by quaternary enhancement: Does Hemoglobin Ypsilanti represent an allosteric intermediate? *Proteins 14*, 351−362.
20. Doyle, M. L., Lew, G., Turner, G. J., Rucknagel, D., and Ackers, G. K. (1992) *Proteins: Struct., Funct., Genet. 14*, 351−362.
21. Doyle, M. L., and Ackers, G. A. (1992) Cooperative Oxygen Binding, Subunit Assembly, and Sulfhydryl Reaction Kinetics of the Eight Cyanomet Intermediate Ligation States of Human Hemoglobin. *Biochemistry 31*, 11182−11195.
22. Kilmartin, J. V., Hewitt, J. A., and Wootton, J. F. (1975) Alteration of functional properties associated with the change in Quaternary structure in unliganded haemoglobin. *J. Mol. Biol. 93*, 203−218.
23. Imai, K. (1973) Analysis of oxygen equilibria of native and chemically modified human adult hemoglobins on the basis of Adair's stepwise oxygenation theory and the allosteric model of Monod, Wyman, and Changeux. *Biochemisry 12*, 798−808.
24. Imai, K. (1973) Correlation between narrow banded ultraviolet spectra and oxygen equilibrium functions in native and chemically modified human hemoglobins. *Biochemistry 12*, 128−134.
25. Imai, K. (1982) *Allosteric Effects in Hemoglobin*, Cambridge University, Press, London.
26. Shibayama, N., Morimoto, H., and Kitagawa, T. (1986) Properties of Chemically Modified Ni(II)-Fe(II) Hybrid Hemoglobins Ni(II) Protoporphyrin IX as a Model a Model for a Permanent Deoxy-heme. *J. Mol. Biol. 192*, 331−336.
27. Shibayama, N., Morimoto, H., and Miyazaki, G. (1986) Oxygen Equilibrium Study and Light Absorption Spectra of Ni(II)-Fe(II) Hybrid Hemoglobins *J. Mol. Biol. 192*, 323−329.
28. Antonini, E., and Brunori, M. (l97l) *Hemoglobins and Myoglobins in their Reactions with Ligands*, Am Elsevier Co., NY.
29. Kwiatkowski, L., and Noble, R. W. (1982) The Effect of the 146β Histidine on the pH Dependence of the R State of Human Hemoglobin. In *Hemoglobin and Oxygen Binding* (Chien, H., Ed.) Elsevier Biochemical.
30. Henry, E. R., Jones, C. M., Hofrichter, J., and Eaton, W. A. (1997) Can a Two State Model MWC Model Explain Hemoglobin Kinetics? *Biochemistry 36*, 6511−6528.
31. Gibson, Q. H. (1999) Kinetics of Oxygen Binding to Hemoglobin A. *Biochemistry 38*, 5191−5199.
32. Alpert, B., El Mohsni, S., Lindqvist, J., and Tfibel, F. (1979) *Chem. Phys. Lett. 64*, 11−16.
33. Duddell, D. A., Morris, R. J., and Richards, J. T. (1979) *J. Chem. Soc., Chem. Commun*. 75−76.
34. Friedman, J. M., and Lyons, K. B. (1980) Transient Raman study of CO-haemoprotein photolysis: origin of the quantum yield. *Nature 284*, 570−572.
35. Chernoff, D. A., Hochstrasser, R. M., and Steele, A. W. (1980) Geminate recombination oxygen and hemolgobin. *Proc. Natl. Acad. Sci. U.S.A. 77*, 5606−5610.
36. Hofrichter, J., Sommer, J. H., Henry, E. R., and Eaton, W. A. (1983) Nanosecond absorption spectroscopy of hemoglobin, elementary processes in kinetic cooperativity. *Proc. Natl. Acad. Sci U.S.A. 80*, 2235−2239.
37. Campbell, B. F., Magde, D., and Sharma, V. S. (1984) Geminate Recombination in Carboxy Hemoglobin A and its Relation to Overall Carbonmonoxide Reactivity. *J. Mol. Biol. 178*, 143−150.

38. Friedman, J. M., Scott, T. W., Fisanick, G. J., Simon, S. R., Findsen, E. W., Ondrias, M. R., and MacDonald, V. W. (1985) Localized Control of Ligand Binding in Hemoglobin: Effect of Tertiary Structure on Picosecond Geminate Recombination. *Science 229*, 187−190.
39. Friedman, J. M. (1985) Structure, Dynamics, and Reactivity in Hemoglobin. *Science 228*, 1273−1280.
40. Marden, M. C., Hazard, E. S., Kimble, C., and Gibson, Q. H. (1987) Geminate ligand recombination as a probe of the R, T equilibrium in hemoglobin. *Eur. J. Biochem. 169*, 611−615.
41. Rousseau, D. L., and Friedman, J. M. (1988) in *Biological Application of Raman Spectroscopy* (Spiro, T. G., Ed.) Vol. III, pp 133−215, Wiley & Sons, New York.
42. Murry, L. P., Hofrichter, J., Henry, E. R., Ikeda-Saito, M., Kitagishi, K., Yonetani, T., and Eaton, W. A. (1988) The Effect of Quaternary Structure on the Kinetics of Conformational Changes and Nanosecond Geminate Rebinding of Carbon Monoxide to Hemoglobin. *Proc. Natl. Acad. Sci. U.S.A. 85*, 2151−2155.
43. Marden, M. C., Kister, J., Bohn, B., and Poyert, C. (1988) T-state hemoglobin with four ligands bound. *Biochemistry 27*, 1659−1664.
44. Kister, J., Poyart, C., and Marden, M. C. (1993) Oxygen and CO binding to Triply NO and Asymmetric No/Co Hemoglobin Hybrids. *Biophys. J. 65*, 1050−1058.
45. Friedman, J. M. (1994) Time-Resolved Resonance Raman Spectroscopy as a Probe of Structure, Dynamics and Reactivity of Hemoglobin. *Methods Enzymol. 232*, 205−231.
46. Peterson, E. S., and Friedman, J. M. (1998) A Possible Allosteric Communication Pathway Identified through a Resonance Raman Study of Four β37 Mutants of Human Hemoglobin A. *Biochemistry 37*, 4346−4357.
47. Huang, J., Juszczak, L. J., Peterson, E. S., Shannon, C., Yang, M., Huang, S., Vidugiris G. V., and Friedman J. M. (1999) The Conformational and Dynamical Basis for Ligand Binding Reactivity in Hemoglobin Ypsilanti (β99 Asp→Tyr): The Origin of the Quaternary Enhancement Effect. *Biochemistry 38*, 4514−4525.
48. Lyons, K. B., and Friedman, J. M. (1982) Dynamics of Carboxyhemoglobin Photolysis. Time Delay Raman Scattering. In *Hemoglobin and Oxygen Binding* (Chien, H., Ed.) Elsevier Biomedical.
49. Scott, T. W., and Friedman, J. M. (1984) Tertiary-Structure Relaxation in Hemoglobin: A Transient Raman Study. *J. Am. Chem. Soc. 106*, 5677−5687.
50. Sassarole, M., and Rousseau, D. L. (1987) Time Dependence of Near-Infrared Spectra of Photodissociated Hemoglobin and Myoglobin. *Biochemistry 26*, 3092−3098.
51. Rodgers, K. R., Su, C., Subramaniam, S., and Spiro, T. G. (1992) Hemoglobin T−R Structure Dynamics From Simultaneous Monitoring of Tyrosine and Tryptophan Time-Resolved UV Resonance Raman Signals. *J. Am. Chem. Soc. 114*, 3697−3709.
52. Jayaraman, V., Rodgers, K. R., Mukerji, I., and Spiro, T. G. (1995) Hemoglobin Allostery: Resonance Raman Spectroscopy of Kinetic Intermediates. *Science 269*, 1843.
53. Goldbeck, R. A., Paquette, S. J., Bjorling, S. C., and Kliger, D. S. (1996) Allosteric intermediates in hemoglobin: Kinetic modeling of HbCO photolysis. *Biochemistry 35*, 8628−8639.
54. Shibayama, N., and Saigo, S. (1995) Fixation of the Quaternary Structures of Human Adult Haemoglobin by Encapsulation in Transparent Porous Silica Gels. *J. Mol. Biol. 251*, 203−209.
55. Bettati, S., and Mozzarelli, A. (1997) T state hemoglobin binds oxygen noncooperatively with allosteric effects of protons, inositol hexaphosphate, and chloride. *J. Biol. Chem. 272*, 32050−32055.
56. Shibayama, N., and Saigo, S. (1999) Kinetics of the Allosteric Transition in Hemoglobin within Silicate Sol−gels. *J. Am. Chem. Soc. 121*, 444−445.
57. Shibayama, N. (1999) Functional analysis of hemoglobin molecules locked in doubly liganded conformations. *J. Mol. Biol. 285*, 1383−1388.
58. Das, T. K., Khan, I., Rousseau, D. L., and Friedman, J. M. (1999) Temperature-dependent quaternary state relaxation in sol−gel encapsulated hemoglobin. *Biospectroscopy 5*, S64−S70.
59. Juszczak, L. J., and Friedman, J. M. (1999) UV resonance Raman spectra of ligand binding intermediates of sol−gel encapsulated hemoglobin. *J. Biol. Chem. 274*, 30357−30360.
60. Khan, I., Shannon, C. F., Dantsker, D., Friedman, A. J., Perez-Gonzalez-de-Apodaca, J., and Friedman, J. M. (2000) Sol−gel Trapping of Functional Intermediates of Hemoglobin: Geminate and Bimolecular Recombination Studies. *Biochemistry* (in press).
61. Ellerby, L. M., Nishida, C. R., Nishida, F., Yamanaka, S. A., Dunn, B., Valentine, J. S., and Zink, J. I. (1992) Encapsulation of proteins in transparent porous silicate glasses prepared by the sol−gel method. *Science 255*, 1113−1115.
62. Acharya, A. S., Sussman, L. G., and Manning, J. M. (1983) *J. Biol. Chem. 258*, 2296−2302.
63. Ampulski, R. S., Ayers, V. E., and Morell, S. A. (1969) *Anal. Biochem. 32*, 163−169.
64. Samuni, U., Navati, M. S., Juszczak, L. J., Dantsker, D., Yang, M., and Friedman, J. M. (2000) *J. Phys. Chem. B 104*, 10802−10813.
65. Ondrias, M. R., Rousseau, D. L., Shelnutt, J. A., and Simon, S. R. (1982) Quaternary Transformation induced changes at the heme in deoxyhemoglobins. *Biochemistry 21*, 3428−3437.
66. Dave, B. C., Dunn, B., Valentine, J. S., and Zink, J. I. (1994) Sol−gel encapsulation methods for biosensors. *Anal. Chem. 66*, 1120A−1127A.
67. Gill, I., and Ballesteros, A. (2000) Bioencapsulation within synthetic polymers: sol−gel encapsulated biologicals. *Trends Biotechnol. 18*, 282−296.
68. Findsen, E. W., Friedman, J. M., and Ondrias, M. R. (1988) Effect of Solvent Viscosity on the Heme-Pocket Dynamics of Photolyzed (Carbonmonoxy) hemoglobin. *Biochemistry 27*, 8719−8724.
69. Huang, J., Ridsdale, A., Wang, J., and Friedman, J. M. (1997) Kinetic Hole Burning, Hole Filling and Conformational Relaxation in Hemeproteins: Direct Evidence for the Functional Significance of a Hierarchy of Dynamical Processes *Biochemistry 36*, 14353−14363.
70. Friedman, J. M., Campbell, B. F., and Noble, R. W. (1990) A possible new control mechanism suggested by resonance Raman spectra from a deep ocean fish hemoglobin. *Biophys. Chem. 37*, 43−59.
71. Agmon, N., and Hopfield, J. J. (1983) CO binding to heme proteins: A model for barrier eight distributions and slow conformational changes. *J. Chem. Phys. 79*, 2042−2053.
72. Coletta, M., Angeletti, M., Ascenzi., P., Bertollini, A., Della Longa, S., De Sanctis, G., Priori, A. M., Santucci, R., and Amiconi, G. (1999) Coupling of the oxygen linked interaction energy for inositol hexaphosphate and bezafibrate binding to human HbA. *J. Biol. Chem. 274*, 6865−6874.
73. Gottfried, D. S., Manjula, B. N., Malavalli, A., Acharya, A. S., and Friedman, J. M. (1999) Probing the diphosphoglycerate binding pocket of HbA and HbPresbyterian (β108Asn→Lys). *Biochemistry 38*, 11307−11315.
74. Fernandez, E. J., Abad-Zapatero. C., and Olsen, K. W. (2000) Crystal structure of Lys$\beta_1$82-Lys$\beta_2$82 cross-linked hemoglobin: A possible allosteric intermediate. *J. Mol. Biol. 290*, 1239−1250.
75. Srajer, V., Reinisch, L., and Champion, P. M. (1988) Protein fluctuations, distributed coupling, and the binding of ligands to heme proteins. *J. Am. Chem. Soc. 110*, 6656−6669.
76. Findsen, E. W., Friedman, J. M., Ondrias, M. R., and Simon, S. R. (1985) Picosecond Time-Resolved Resonance Raman Studies of Hemoglobin: Implications for Reactivity. *Science 229*, pp 661−665.
77. Franzen, S., Bohn, B., Poyart, C., DePillis, G., Boxer, S. G., and Martin, J.−L. (1995) Functional Aspects of Ultra-rapid Heme Doming in Hemoglobin, Myoglobin, and the Myoglobin Mutant H93G. *J. Biol. Chem. 270*, 1718−1720.

78. Franzen, S., Lambry, J. C., Bohn, B., Poyart, C., and Martin, J. L. (1994) Direct evidence for the role of haem doming as the primary event in the cooperative transition of haemoglobin. *Nat. Struct. Biol. 1*, 230−233.
79. Dasgupta, S., and Spiro, T. G. (1986) Resonance Raman characterization of the 7-ns photoproduct of(carbonmonoxy)-hemoglobin: implications for hemoglobin dynamics. *Biochemistry 25*, 5941−5948.
80. Friedman, J. M., Rousseau, D. L., Ondrias, M. R., and Stepnoski, R. A. (1982) Transient Raman Study of Hemoglobin: Structural Dependence of the Iron- Histidine Linkage. *Science 218*, 1244−1246.
81. Friedman, J. M., Scott, T. W., Stepnoski, R. A., Ikeda-Saito, M., and Yonetani, T. (1983) The Iron-Proximal Histidine Linkage and Protein Control of Oxygen Binding in Hemoglobin. *J. Biol. Chem. 258*, 10584.
82. Ho, C. (1992) Proton Nuclear Magnetic Resonance Studies on Hemoglobin: Cooperative Interactions and Partially Ligated Intermediates. *Adv. Protein Chem. 43*, 154−312.
83. Englander, J. J., Godfrey, L., McKinnie, R. E., and Englander, S. W. (1998) Energetic components of the allosteric machinary measured by hydrogen exchange. *J. Mol. Biol. 284*, 1695−1706.
84. Englander, J. J., Rumbley, J. N., and Englander, S. W. (1998) Signal transmission between subunits in the hemoglobin T state. *J. Mol. Biol. 284*, 1707−1716.
85. Bettati, S., Kwiatkowski, L. D., Kavanaugh, J. S., Mozzarelli, A., Arnone, A., Rossi, G. L., and Noble., R. W. (1997) Structure and oxygen affinity of crystalline des-His 146β human hemoglobin in the T state. *J. Biol. Chem. 272*, 33077−33084.
86. Wang, D., and Spiro, T. G. (1998) Structure Changes in Hemoglobin upon Deletion of C−Terminal Residues, Monitored by Resonance Raman Spectroscopy. *Biochemistry 37*, 9940−9951.
87. Dick, L. A., Heibel, G., Moore, E. G., and Spiro, T. G. (1999) UV resonance Raman spectra reveal a structural basis for diminished proton and CO2 binding to $\alpha\alpha$ cross linked hemoglobin. *Biochemistry 38*, 6406−6410.
88. Hu, X., Rodgers, K. R., Mukerji, I., and Spiro, T. G. (1999) New light on allostery: dynamic resonance Raman spectroscopy on hemoglobin Kempsey. *Biochemistry 38*, 3462−3467.
89. Chan, N.-L., Rogers, P. H. and Arnone, A, (1998) Crystal structure of the S-nitroso form of the liganded human hemoglobin. *Biochemistry 37*, 16459−16464.

BI010051O